Photon Counting CT
Detectors, Prototypes and Scan Modes

Marc Kachelrieß

German Cancer Research Center (DKFZ)
Heidelberg, Germany
www.dkfz.de/ct

DEUTSCHES
KREBSFORSCHUNGSZENTRUM
IN DER HELMHOLTZ-GEMEINSCHAFT

Indirect Conversion (Today)

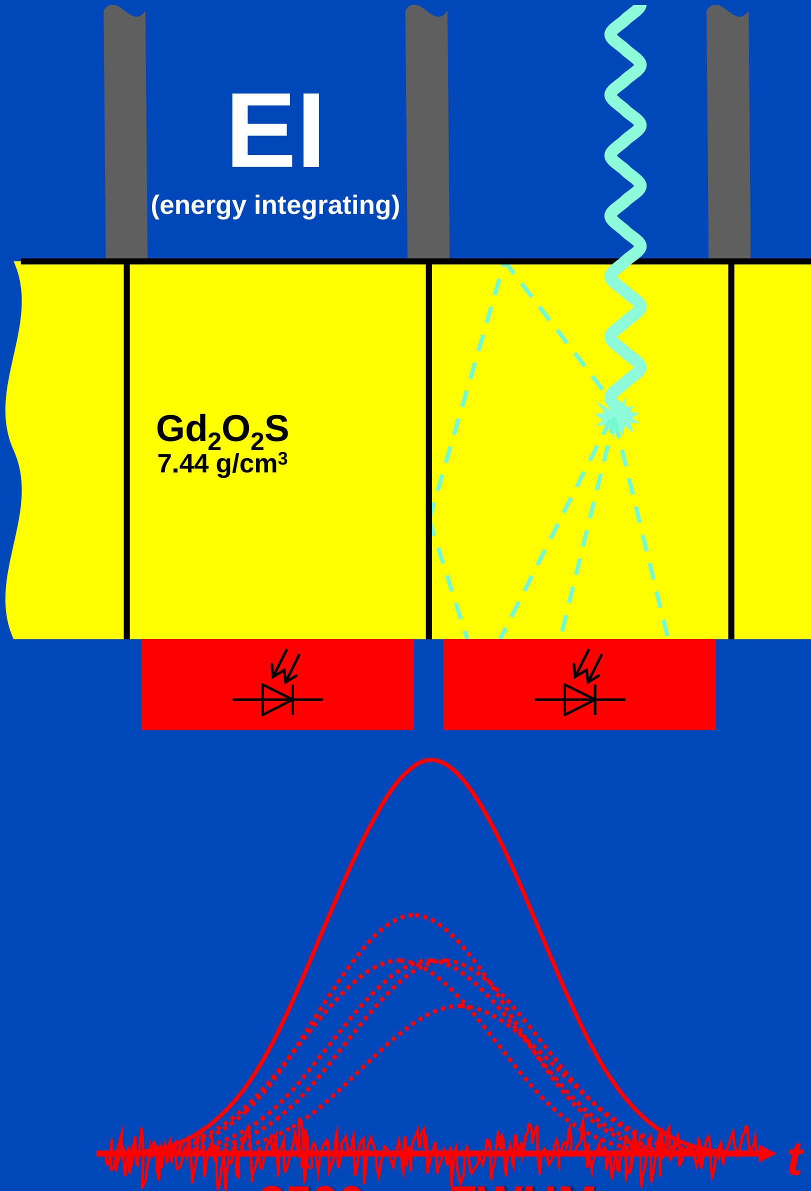

2500 ns FWHM

i.e. max $O(40 \cdot 10^3)$ cps

Direct Conversion (Future)

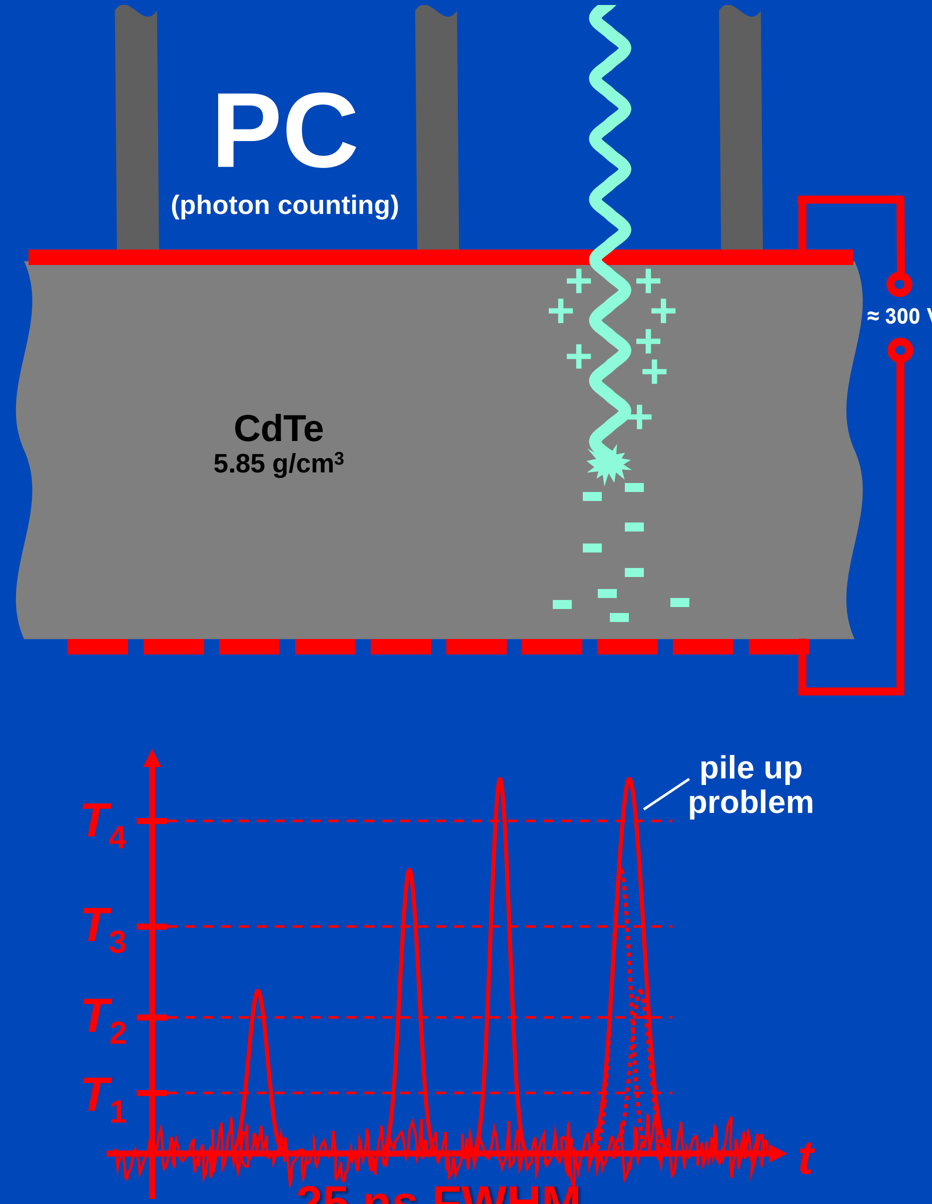

25 ns FWHM

i.e. max $O(40 \cdot 10^6)$ cps

Requirements for CT: up to 10^9 x-ray photon counts per second per mm². Hence, photon counting only achievable for direct converters.

Dark Image of Photon Counter Shows Background Radiation

18 frames, 5 min integration time per frame

Events per Frame

Energy Integrating (Dexela)

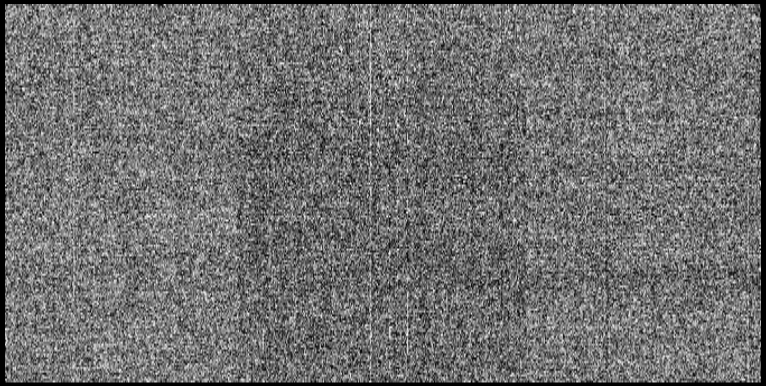

C/W = 0 a.u./70 a.u.

Photon Counting (Dectris Santis)

C/W = 1 cnts/2 cnts

Energy-Selective Detectors: Improved Spectroscopy, Reduced Dose?

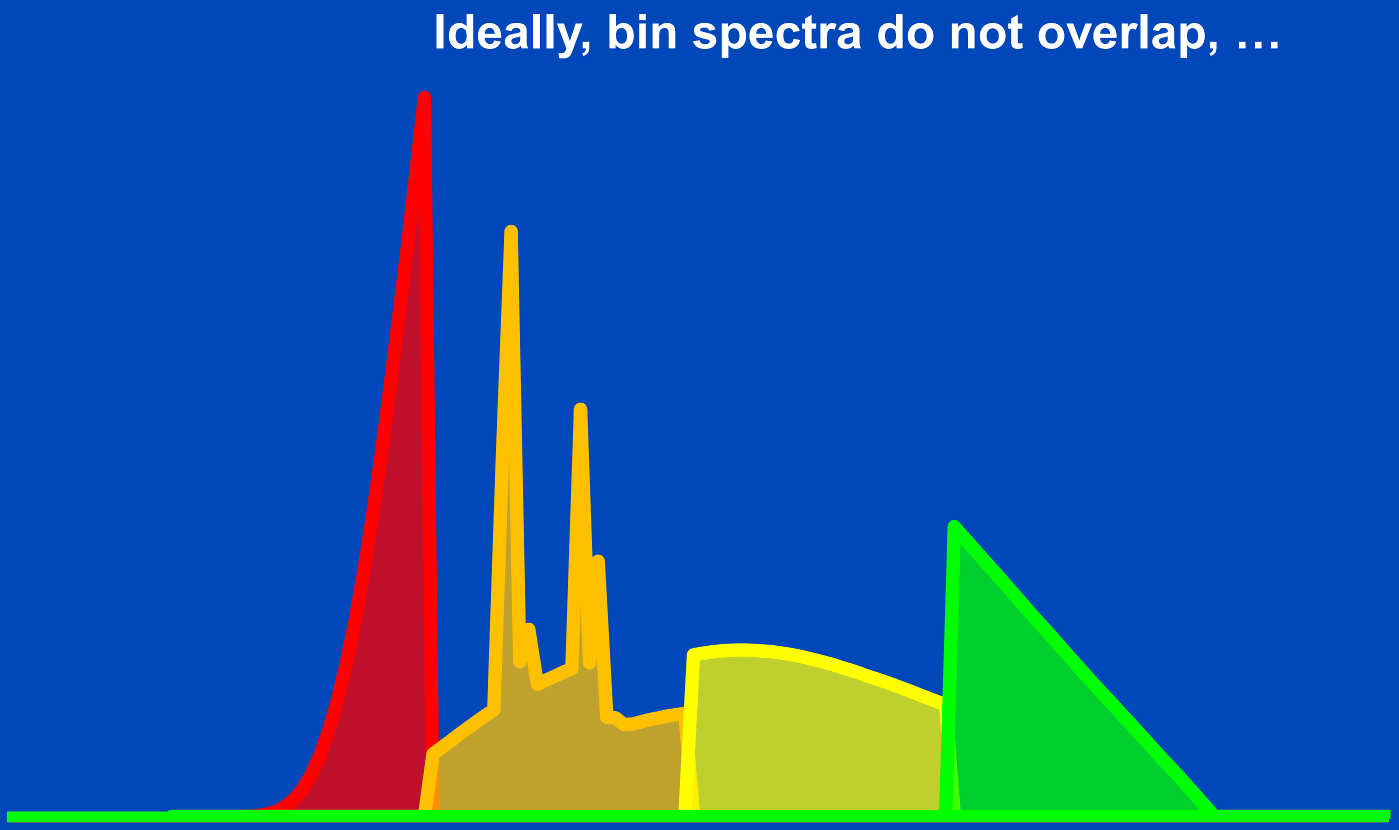

Spectra as seen after having passed a 32 cm water layer.

Energy-Selective Detectors: Improved Spectroscopy, Reduced Dose?

… realistically, however they do!

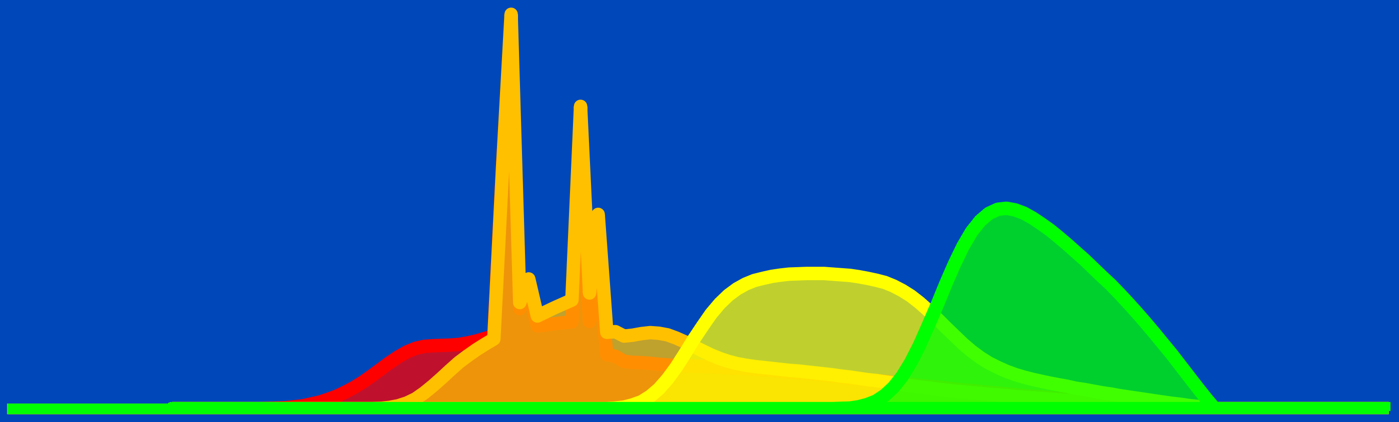

Spectra as seen after having passed a 32 cm water layer.

Photon Events

- Detection process in the sensor
- Photoelectric effect (e.g. 80 keV)

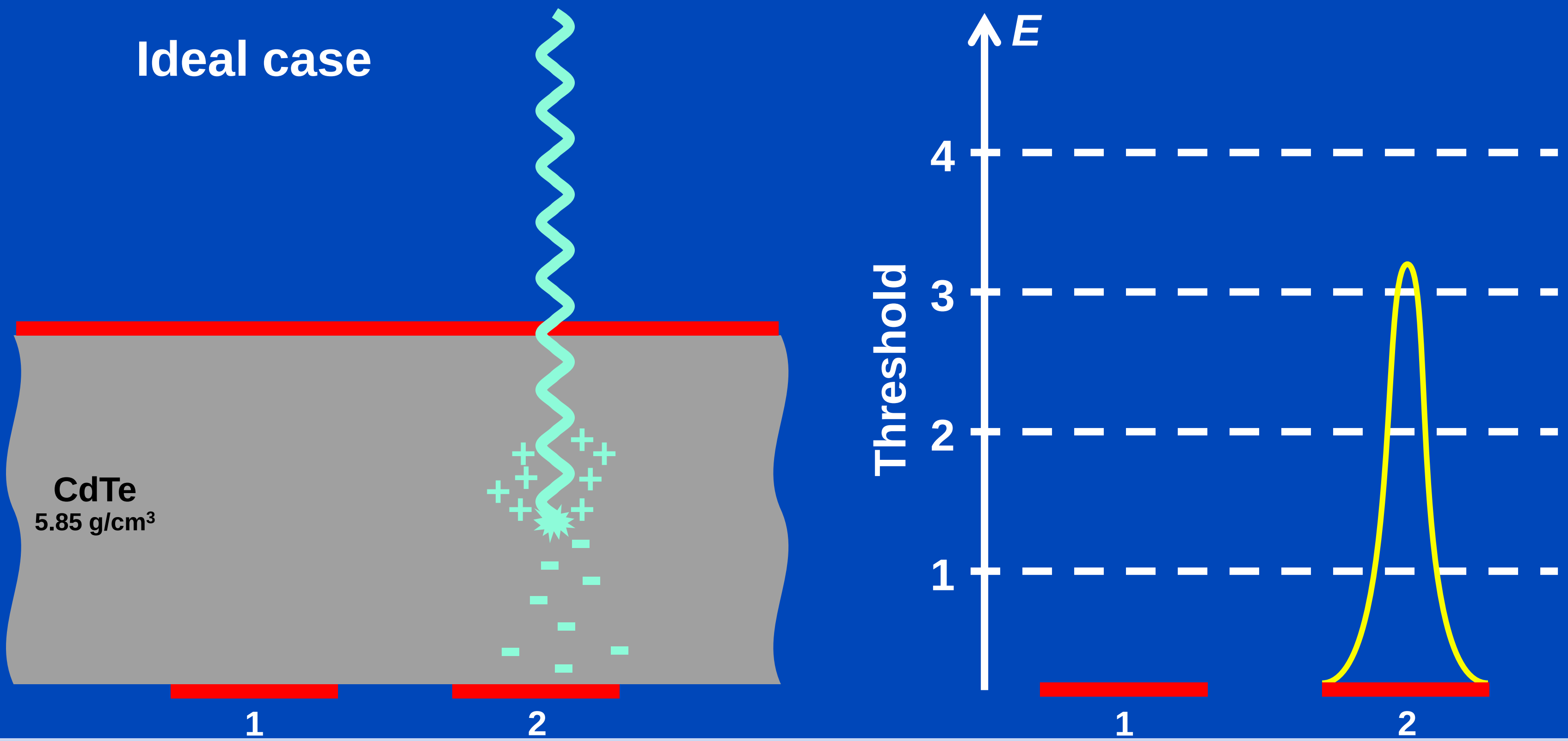

Photon Events

- Detection process in the sensor
- Compton scattering or K-fluorescence (e.g. 80 keV)

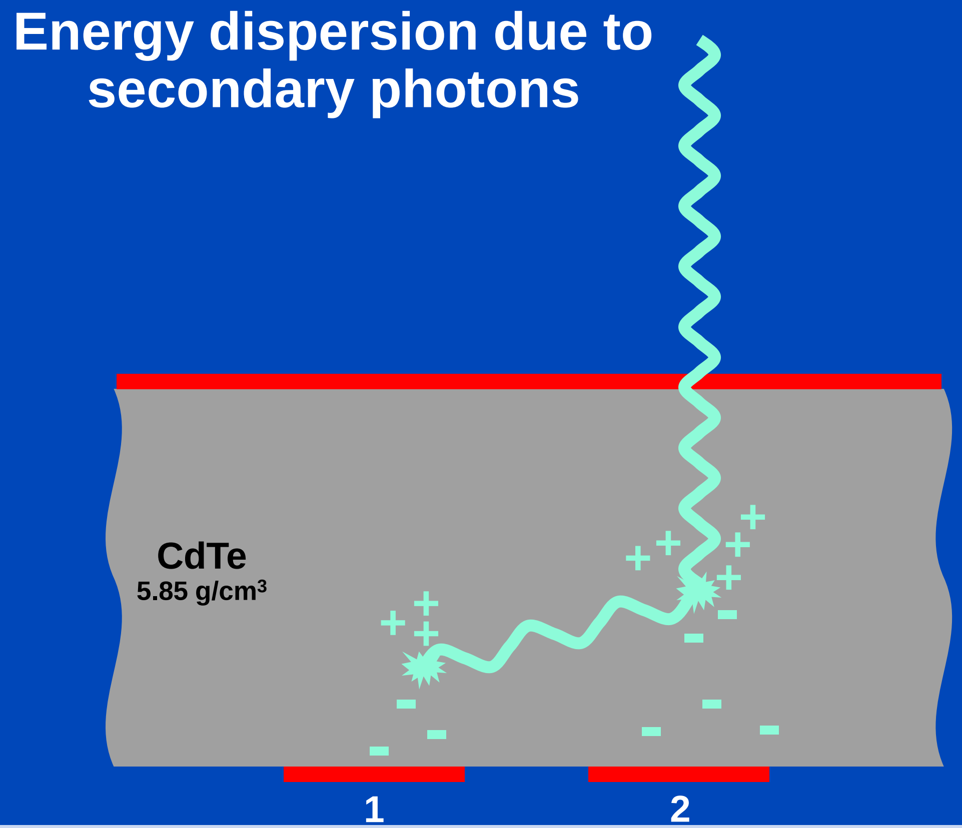

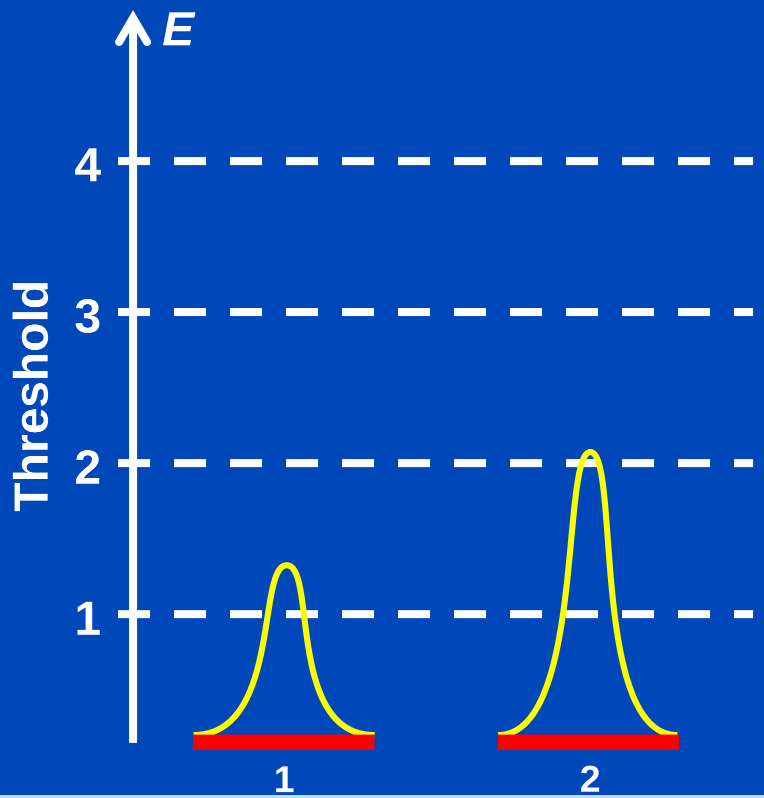

Photon Events

- Detection process in the sensor
- Photoelectric effect (e.g. 30 keV), charge sharing

Energy dispersion due to charge diffusion

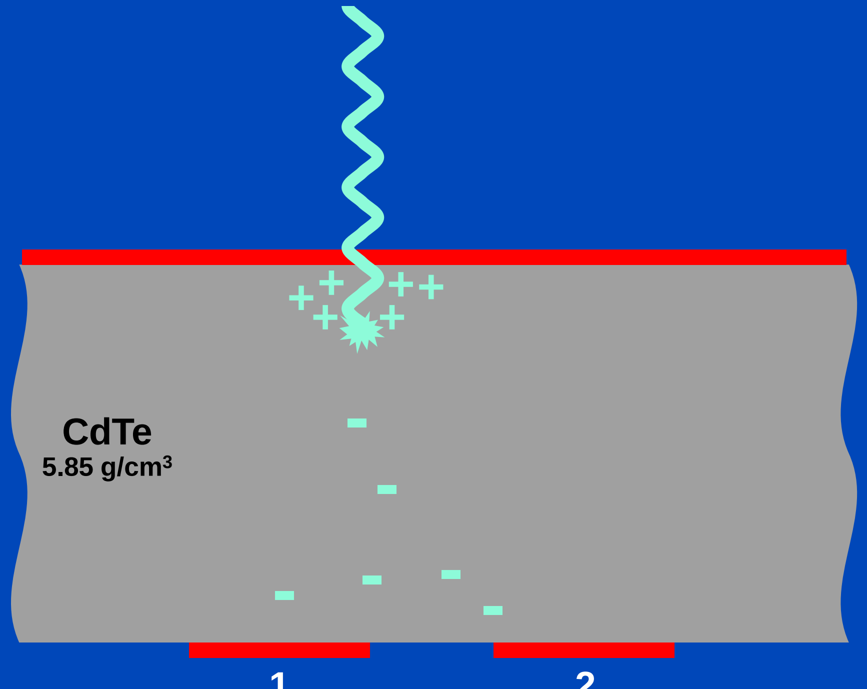

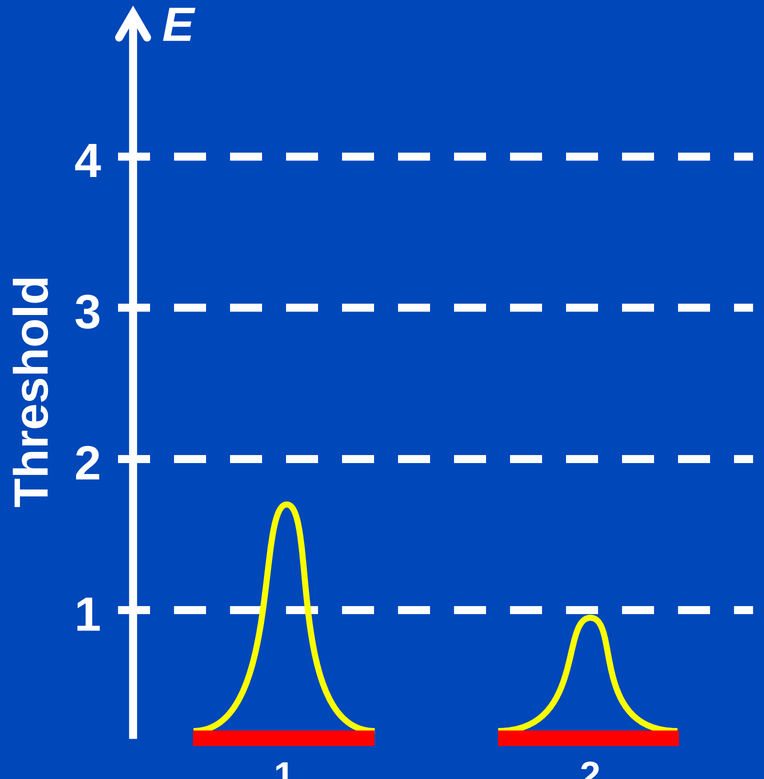

Potential Advantages of Photon Counting CT

- No electronic noise
  - Less dose for infants
  - Less noise for obese patients
- Counting
  - Swank factor = 1 = maximal
  - Higher weights on low energies = good for iodine contrast
- Energy bin weighting
  - Lower dose/noise
  - Improved iodine CNR
- Smaller pixels (to avoid pileup)
  - Higher spatial resolution
  - Lower dose/noise at conventional resolution
- Spectral information on demand

What We Want

- High count rate
- Small detector pixels
- Good spectral separation
- Low cross-talk
- Large detector areas
- High absorption
- Low costs

Part 1: Existing Systems

Existing Systems 2018

Willemink et al

Table 2: Current Photon-counting CT Projects Targeted Toward Full-Body Clinical CT

Project	Detector Material*	Detector Element Size (mm^2)†	Current Status	Reference
GE Healthcare (Chicago, Ill)/ Stanford University (Stanford, Calif)/Rensselaer Polytechnic Institute (Troy, NY) high-dose efficiency CT	CZT, planned integration with dynamic bowtie	0.5 × 0.5	Table-top system under construction at Rensselaer Polytechnic Institute	29
Medipix All Resolution System (MARS Bioimaging, Christchurch, New Zealand)	CZT	0.11 × 0.11	Imaging of specimens and small animals. Human-size scanner under construction.	30
Philips Healthcare (Best, the Netherlands) spectral photon-counting CT	CZT	0.5 × 0.5	Imaging of specimens and small animals. Prototype system with small detector installed in human-sized gantry in Lyon, France.	31,32
KTH Royal Institute of Technology (Stockholm, Sweden)/Prismatic Sensors (Stockholm, Sweden) silicon strip	Silicon	0.5 × 0.4	Table-top measurements at KTH Royal Institute of Technology	5
Siemens (Forchheim, Germany) dual detector	Dual-source CT with one CdTe photon-counting detector	0.225 × 0.225, detector elements binned into macro mode (0.9 × 0.9) and sharp mode (0.45 × 0.45)	Prototype human-size systems installed at Mayo Clinic (Rochester, Minn), at National Institutes of Health (Bethesda, Md), and in Forchheim, Germany. Research imaging of human volunteers	33

* CdTe = cadmium telluride, CZT = cadmium zinc telluride.

† Detector element sizes are the actual physical sizes, that is, not rescaled to isocenter.

Willemink et al. Radiology, 289(2):293-312, 2018

Existing Systems 2020

	Setup	Detector	Pixel size (mm^2)	FOV	Thresholds	Acquisition	Extra
Philips Healthcare (preclinical) [1, 2, 3]	Preclinical	CdZnTe	0.5 × 0.5	16.8 cm	5 (30-98 keV)	2400 fps	
MARS Bioimaging (preclinical) [4, 5]	Preclinical MARS orthopaedic imaging-cooming soon	2 mm CdZnTe; five medipix3RX chips in a row (70 mm × 14 mm)	0.11 × 0.11	10 cm	8 (10-120 keV)	Scan time: 8 min for a sample with 30 mm diameter and 15 mm length	Charge summing mode
Siemens Somaton CounT [6]	**Clinical, whole body**	Dual-source CT with one PC detector of 1.6 mm CdTe	0.225 × 0.225 or 0.45 × 0.45 or 0.9 × 0.9	**27.5 cm**	4 (20-90 keV)	2304 fps 4608 fps	
KTH Royal Institute of Technology, Stockholm [7]	Table-top Translating detector	30 mm silicon strip	0.4 × 0.5	0.93 cm (need to translate the detector several times)	8	300 $Mcps/mm^2$	Edge-on design
Center for In Vivo Microscopy, Duke University, Durham (preclinical) [8, 9]	Preclinical Table-top	1 mm CdTe	0.15 × 0.15	~6.5 cm	4		
DKFZ (preclinical)	Preclinical	1 mm CdTe	0.15 × 0.15	~15 cm	4 (9-90 keV)	200 fps 100 $Mcps/mm^2$	

dkfz.

[1] Muenzel, et al. (2017). Spectral Photon-counting CT: Initial Experience with Dual–Contrast Agent K-Edge Colonography. Radiology.
[2] Si-Mohamed, et al. (2017). Evaluation of spectral photon counting computed tomography K-edge imaging for determination of gold nanoparticle biodistribution: In vivo. Nanoscale.
[3] Si-Mohamed, et al. (2017). Review of an initial experience with an experimental spectral photon-counting computed tomography system. Nuclear Instruments and Methods in Physics Research Section A
[4]Ostadhossein, (2020). Multi-“Color” Delineation of Bone Microdamages Using Ligand-Directed Sub-5 nm Hafnia Nanodots and Photon Counting CT Imaging. Advanced Functional Materials.
[5] MARS Small Bore Spectral Scanner Brochure: https://www.marsbioimaging.com/mars/wp-content/uploads/2018/07/MARS_Electronic.pdf
[6] Yu, et al. (2016). Evaluation of conventional imaging performance in a research whole-body CT system with a photon-counting detector array. Physics in Medicine and Biology.
[7] Persson, et al. (2014). Energy-resolved CT imaging with a photon-counting silicon-strip detector. Physics in Medicine and Biology.
[8] Badea, et al. (2019). Functional imaging of tumor vasculature using iodine and gadolinium-based nanoparticle contrast agents: a comparison of spectral micro-CT using energy integrating and photon counting detectors. Physics in Medicine and Biology.
[9] Clark, et al. (2019). Photon-counting cine-cardiac CT in the mouse. PLoS ONE.

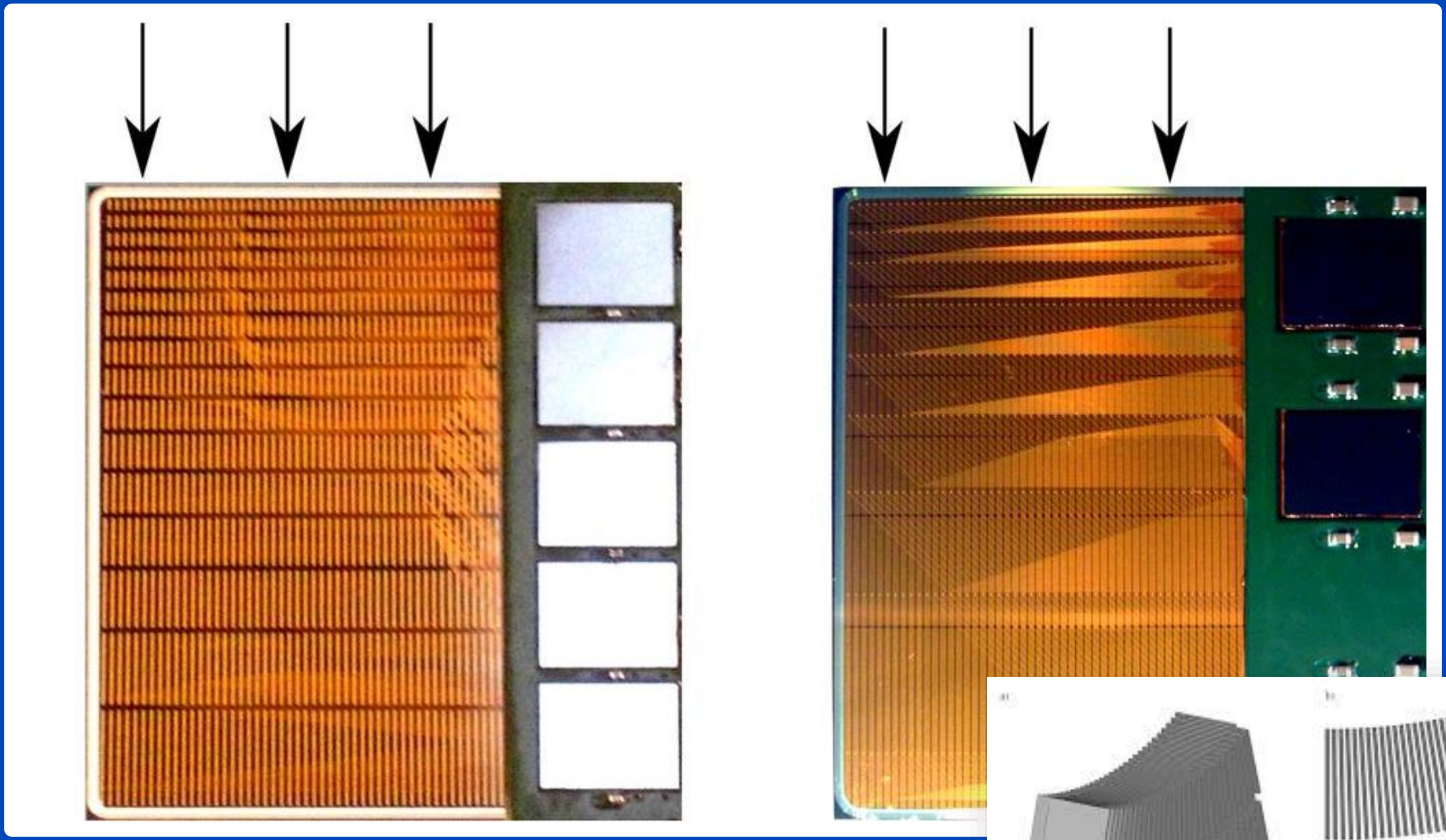

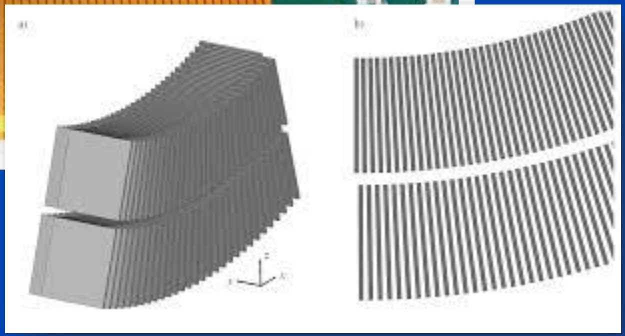

Image courtesy of KTH Royal Institute of Technology

Non-Proprietary Relevant PC Detectors

	Sensor	Pixel	Sensor Area	Bins	Acquisition	Features
Medipix3RX[1,2]	Si or CdTe	55 µm	1.4 × 1.4 cm² 3-side buttable	2	61 Mcps/mm²	Charge summing mode: half the number of thresholds, count rate reduced by a factor of 4 to 5
		110 µm		8	15 Mcps/mm²	
Pixirad Module[3]	CdTe 0.65 mm	55 µm	3.1 × 2.5 cm² 2-side buttable	2	200 fps 162 Mcps/mm²	Hexagonal pixel
Dectris Säntis[4]	CdTe	150 µm	30.8 × 3.8 cm²	4	200 fps 100 Mcps/mm²	
Direct conversion XC Thor[5]	CdTe 0.75 or 2.0 mm	100 µm	up to 5.12 × 40.0 cm²	2	300 fps 200 Mcps/mm²	Charge sharing correction

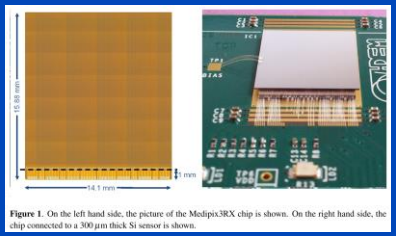

Medipix

Pixirad

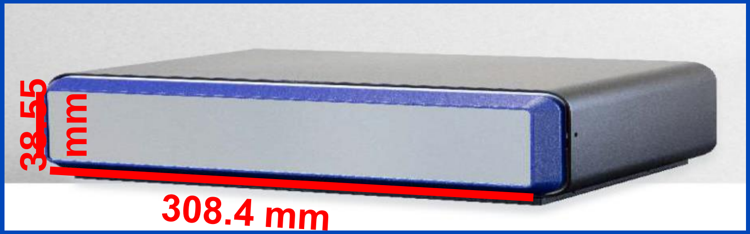

Säntis

XC Thor

[1] Ballabriga, et al. (2013). The medipix3RX: A high resolution, zero dead-time pixel detector readout chip allowing spectroscopic imaging. Journal of Instrumentation.
[2] Frojdh, et al. (2014). Count rate linearity and spectral response of the Medipix3RX chip coupled to a 300µm silicon sensor under high flux conditions. Journal of Instrumentation.
[3] https://indico.cern.ch/event/284070/sessions/53910/attachments/524517/723391/Ravenna_Bellazzini1.pdf
[4] Information provided by Dectris Ltd.
[5] https://directconversion.com/product/xc-thor/

Philips SPCCT

- **The objective of the SPCCT project is to develop and validate a widely accessible, new quantitative and analytical in vivo imaging technology combining Spectral Photon Counting CT and contrast agents, to accurately and early detect, characterize and monitor neurovascular and cardiovascular disease.**

SPCCT
IMAGING ALL THE PHOTONS

Spectral Photon Counting CT European Project announces the arrival and set-up of the Philips prototype spectral scanner designed for human in Lyon.

Lyon, France, February 19, 2019

Philips SPCCT

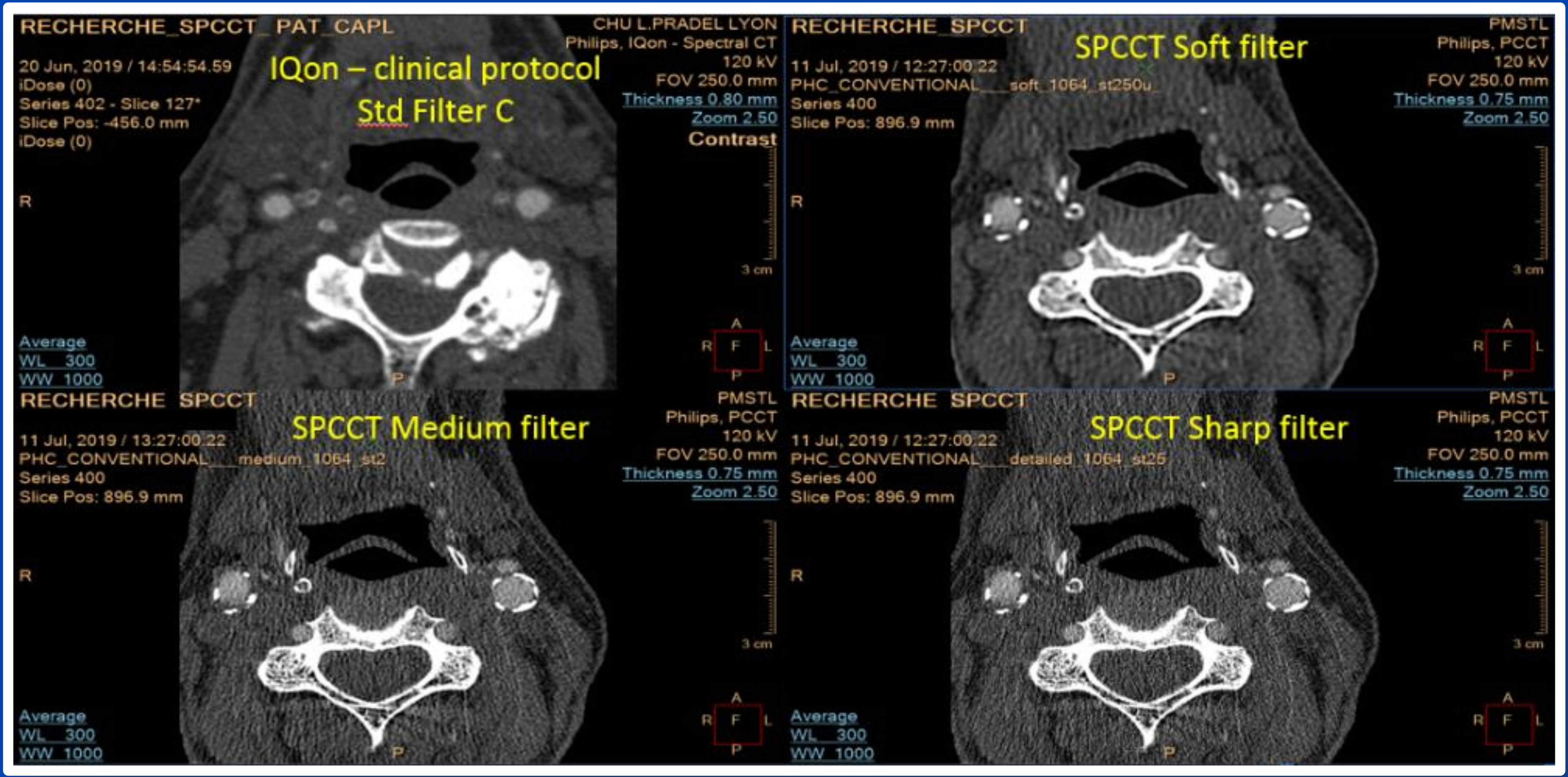

Patient scan before (EI) and after (PC) treatment. www.spcct.eu

Siemens CounT CT System

Gantry from a clinical dual source scanner

A: conventional CT detector (50.0 cm FOV)

B: Photon counting detector (27.5 cm FOV)

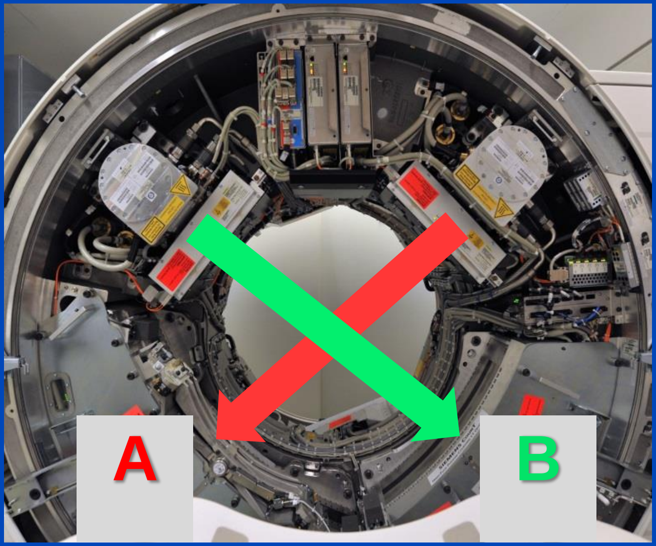

Readout Modes of the CounT

PC-UHR Mode
0.25 mm pixel size

PC-Macro Mode
0.50 mm pixel size

EI detector
0.60 mm pixel size

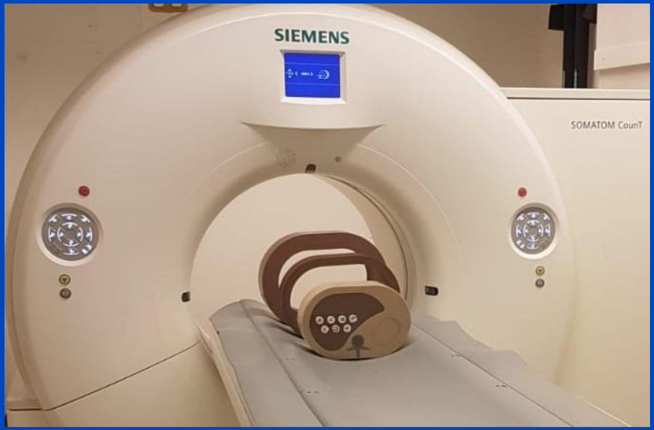

Part 2: Scan Modes

Readout Modes of the Siemens CounT

Macro Mode
0.9 × 1.1 mm focus
2 readouts
16 mm z-coverage

12	12	12	12
12	12	12	12
12	12	12	12
12	12	12	12

Chess Mode
0.9 × 1.1 mm focus
4 readouts
16 mm z-coverage

12	34	12	34
34	12	34	12
12	34	12	34
34	12	34	12

Sharp Mode
0.9 × 1.1 mm focus
5 readouts
12 mm z-coverage

1	1	1	1
1	1	1	1
1	1	1	1
1	1	1	1

2	2	2	2
2	2	2	2
2	2	2	2
2	2	2	2

UHR Mode
0.7 × 0.7 mm focus
8 readouts
8 mm z-coverage

12	12	12	12
12	12	12	12
12	12	12	12
12	12	12	12

1.6 mm CdTe sensor. No FFS on detector B (photon counting detector). 4×4 subpixels of 225 µm size = 0.9 mm pixels (0.5 mm at isocenter). An additional 225 µm gap (e.g. for anti scatter grid) yields a pixel pitch of 1.125 mm.The whole detector consists of 128×1920 subpixels = 32×480 macro pixels.

This photon-counting whole-body CT prototype, installed at the Mayo Clinic, at the NIH and at the DKFZ is a DSCT system. However, it is restricted to run in single source mode. The second source is used for data completion and for comparisons with EI detectors.

CounT Detector Pixel Size EI vs. PC

EI
0.6 mm pixel size

PC Macro or Chess Mode
0.5 mm pixel size

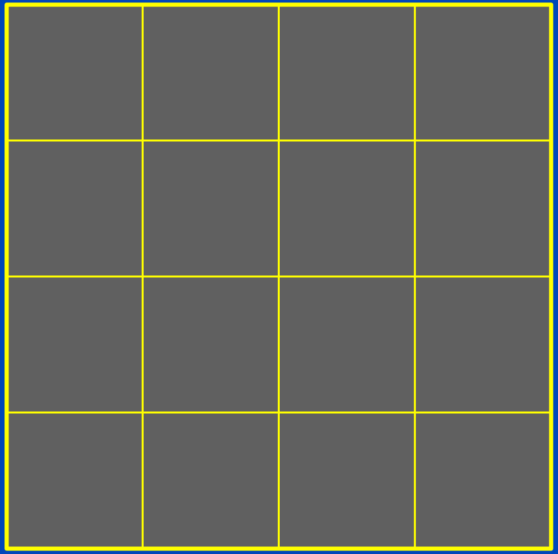

PC UHR Mode
0.25 mm pixel size

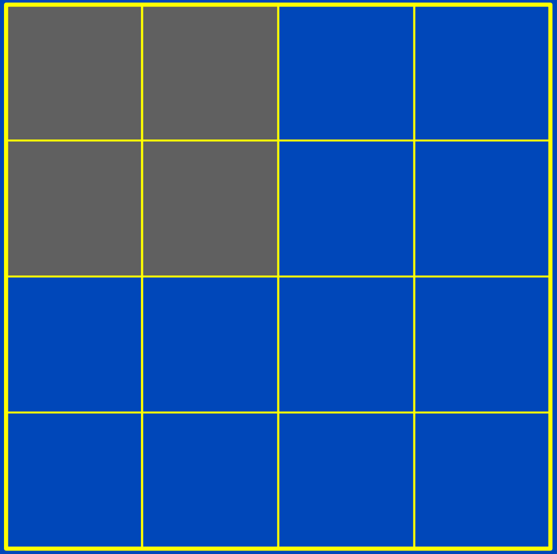

To Bin or not to Bin?
(the continuous view)

This nice phrase was coined by Norbert Pelc.

- **We have** $\mathrm{PSF}(x) = s(x) * a(x)$ **and** $\mathrm{MTF}(u) = S(u)A(u)$.
- **From Rayleigh‘s theorem we find noise is**

$$\sigma^2 = \int dx\, a^2(x) = \int du\, A^2(u) = \int du\, \frac{\mathrm{MTF}^2(u)}{S^2(u)}$$

- **Compare Small (A) with large (B) detector pixels:**

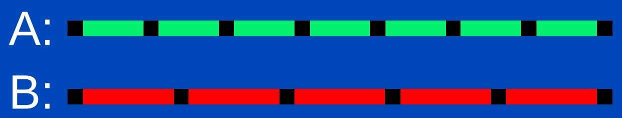

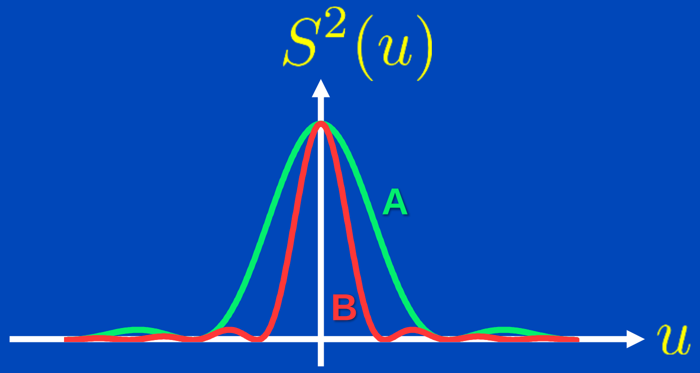

- **We have** $S_\mathrm{A}(u) > S_\mathrm{B}(u)$ **and thus** $\sigma_\mathrm{A}^2 < \sigma_\mathrm{B}^2$.
- **This means that a desired PSF/MTF is often best achieved with smaller detectors.**

Kachelrieß, Kalender. Med. Phys. 32(5):1321-1334, May 2005
Baek, Pineda, and Pelc. PMB 58:1433-1446, 2013

The “Small Pixel Effect”

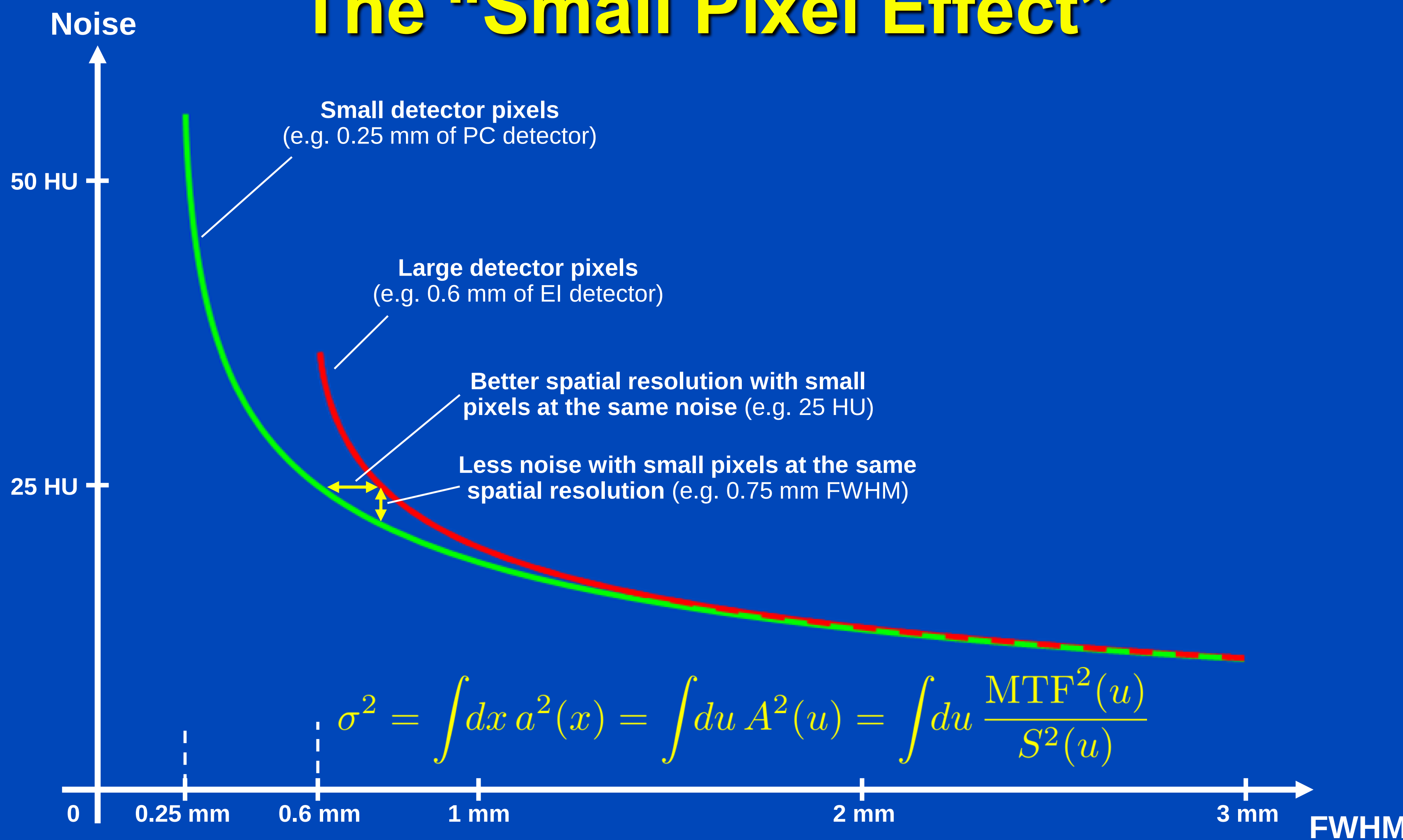

$$\sigma^2 = \int dx\, a^2(x) = \int du\, A^2(u) = \int du\, \frac{\mathrm{MTF}^2(u)}{S^2(u)}$$

CounT Std **CounT HighRes**

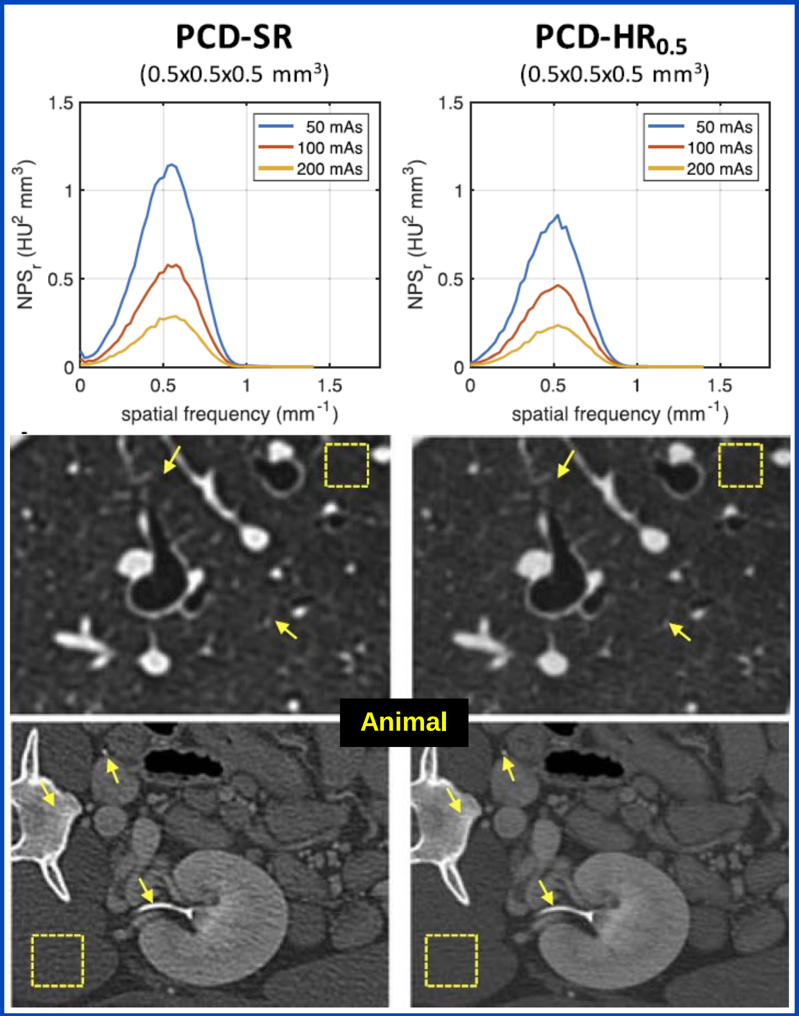

"However, when comparing with standard resolution data at same in-plane resolution and slice thickness, the PCD 0.25 mm detector mode showed **19% less image noise** in phantom, animal, and human scans."

CounT Std **CounT HighRes**

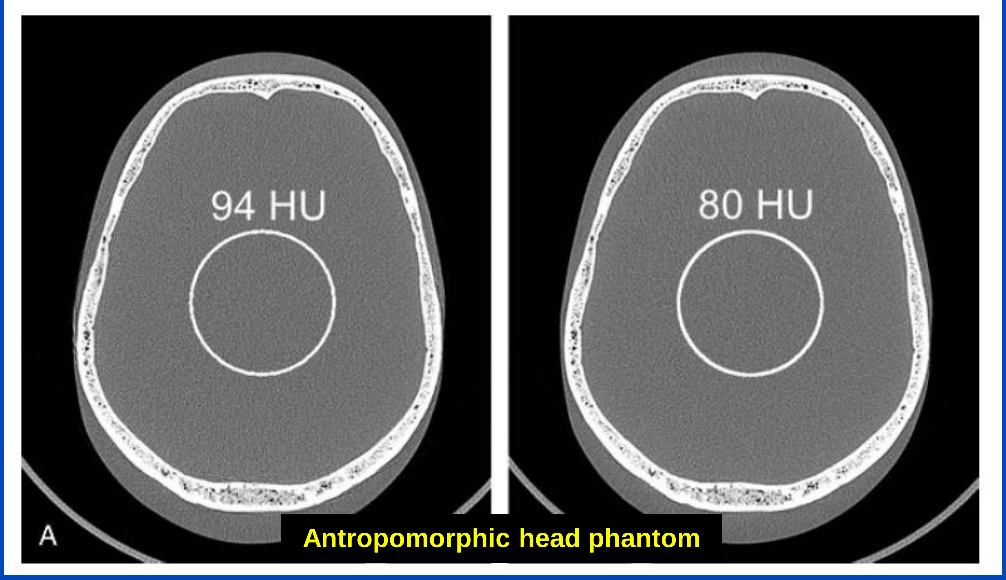

A **15% noise reduction** (from 94 HU to 80 HU) was observed (same spatial resolution and dose). This corresponds to a dose reduction of 28%.

Pourmorteza et al. Dose Efficiency of Quarter-Millimeter Photon-Counting Computed Tomography: First-in-Human Results. Invest. Radiol. 53(6), 2018.

Leng et al. 150 µm Spatial Resolution Using Photon-Counting Detector Computed Tomography Technology. Invest. Radiol. 53(11), 2018

All images reconstructed with 1024^2 matrix and 0.15 mm slice increment.
C = 1000 HU
W = 3500 HU

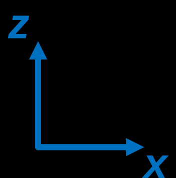

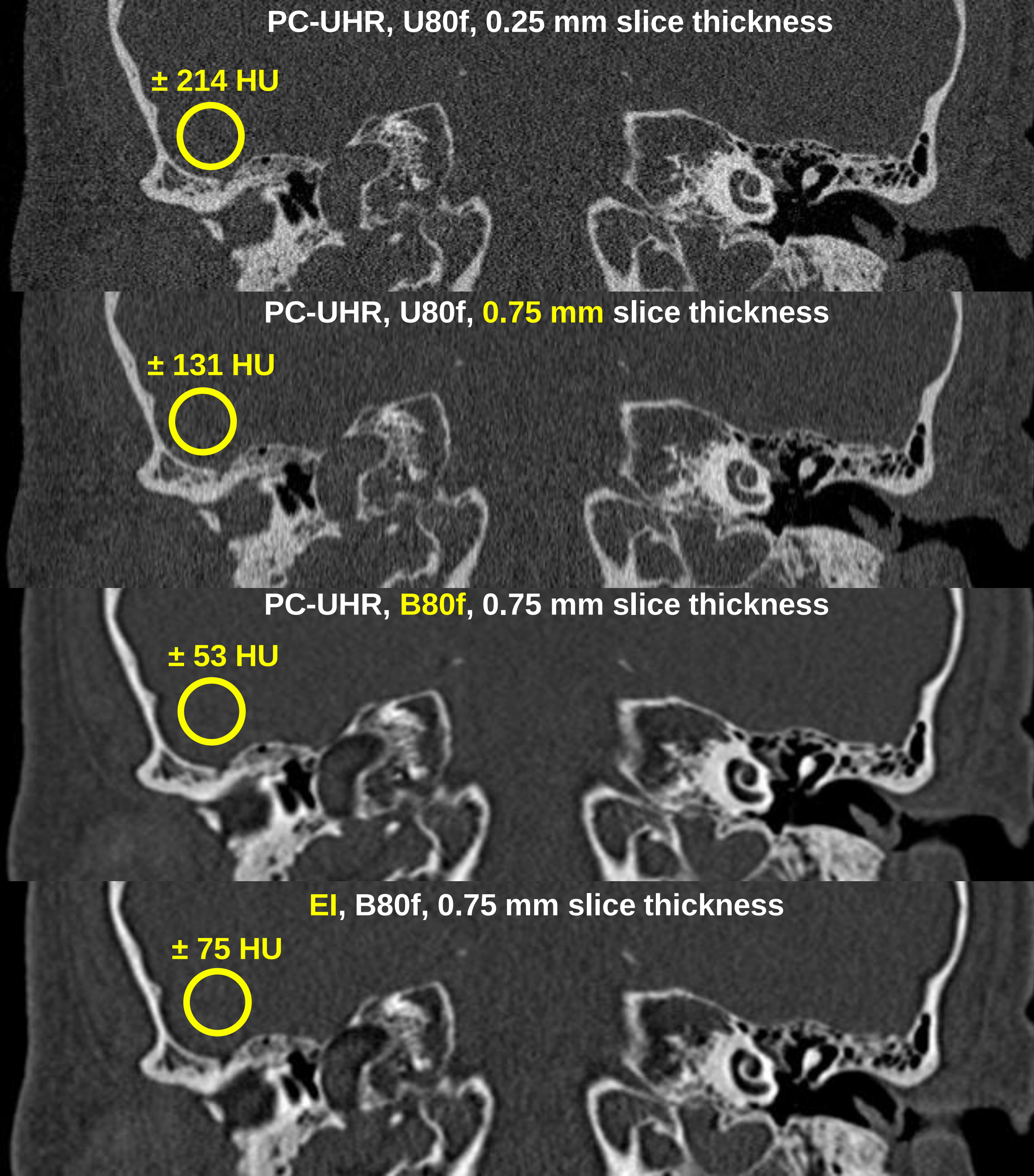

10% MTF: 19.1 lp/cm
10% MTF:17.2 lp/cm
xy FWHM: 0.48 mm
z FWHM: 0.40 mm
$CTDI_{vol}$: 16.0 mGy

10% MTF: 19.1 lp/cm
10% MTF:17.2 lp/cm
xy FWHM: 0.48 mm
z FWHM: 0.67 mm
$CTDI_{vol}$: 16.0 mGy

10% MTF: 9.3 lp/cm
10% MTF:10.5 lp/cm
xy FWHM: 0.71 mm
z FWHM: 0.67 mm
$CTDI_{vol}$: 16.0 mGy

10% MTF: 9.3 lp/cm
10% MTF:10.5 lp/cm
xy FWHM: 0.71 mm
z FWHM: 0.67 mm
$CTDI_{vol}$: 16.0 mGy

Data courtesy of the Institute of Forensic Medicine of the University of Heidelberg and of the Division of Radiology of the German Cancer Research Center (DKFZ)

Acquisitions at same noise

EI, B70f

UHR, B70f

C = 1000 HU
W = 3500 HU

Acquisition with EI:

- Tube voltage of 120 kV
- Tube current of 350 mAs
- Resulting dose of $CTDI_{vol\ 32\ cm}$ = 26.4 mGy

Acquisition with UHR:

- Tube voltage of 120 kV
- Tube current of 200 mAs
- Resulting dose of $CTDI_{vol\ 32\ cm}$ = 16.1 mGy

This is a 39% reduction of dose!

Energy Integrating
(Detected Spectra at 100 kV and 140 kV)

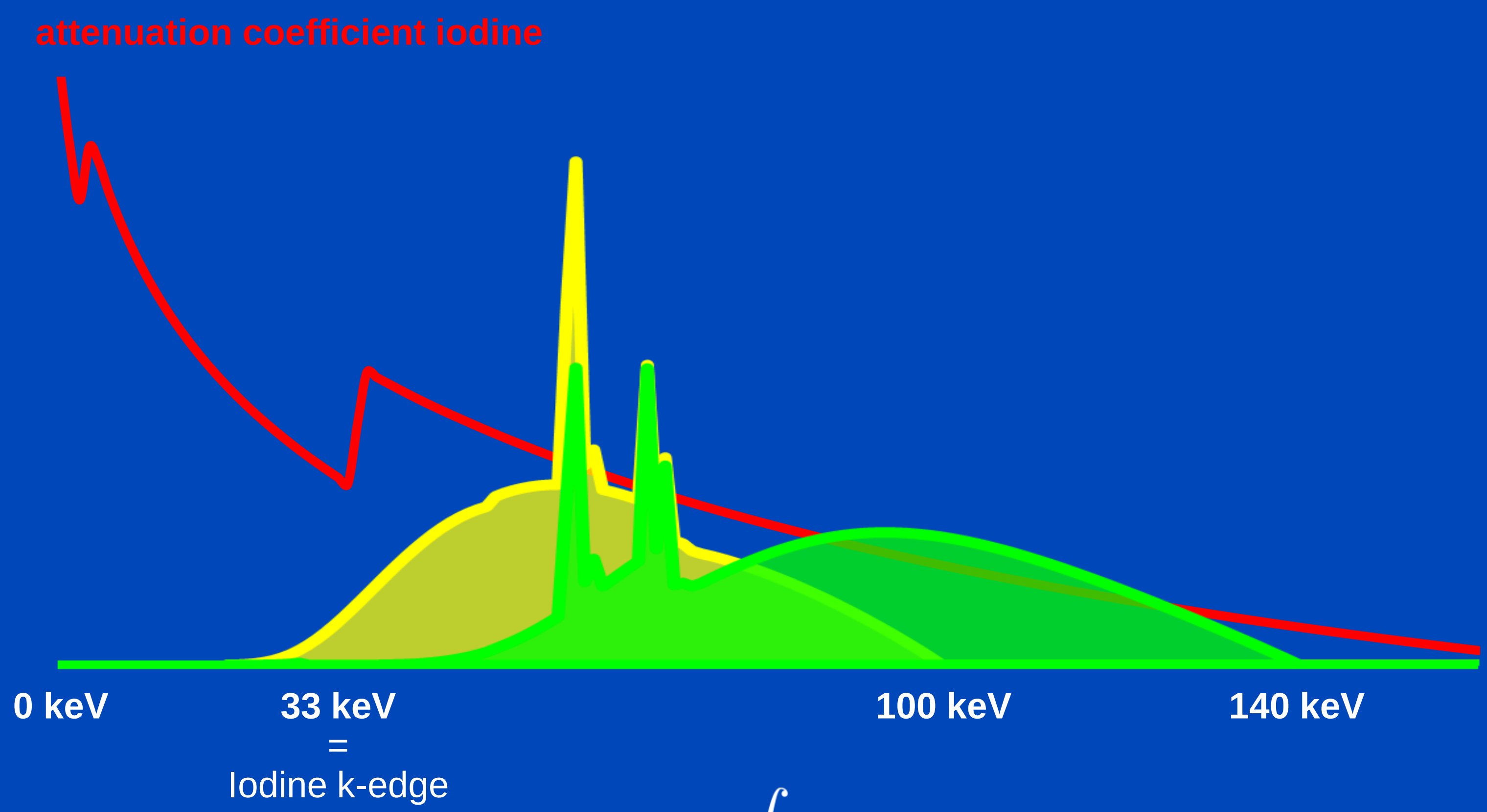

$$\mathrm{Signal}_{\mathrm{EI}} = \int dE\, E\;\; N(E)$$

Photon Counting: "Iodine Effect"
(Detected Spectra at 100 kV and 140 kV)

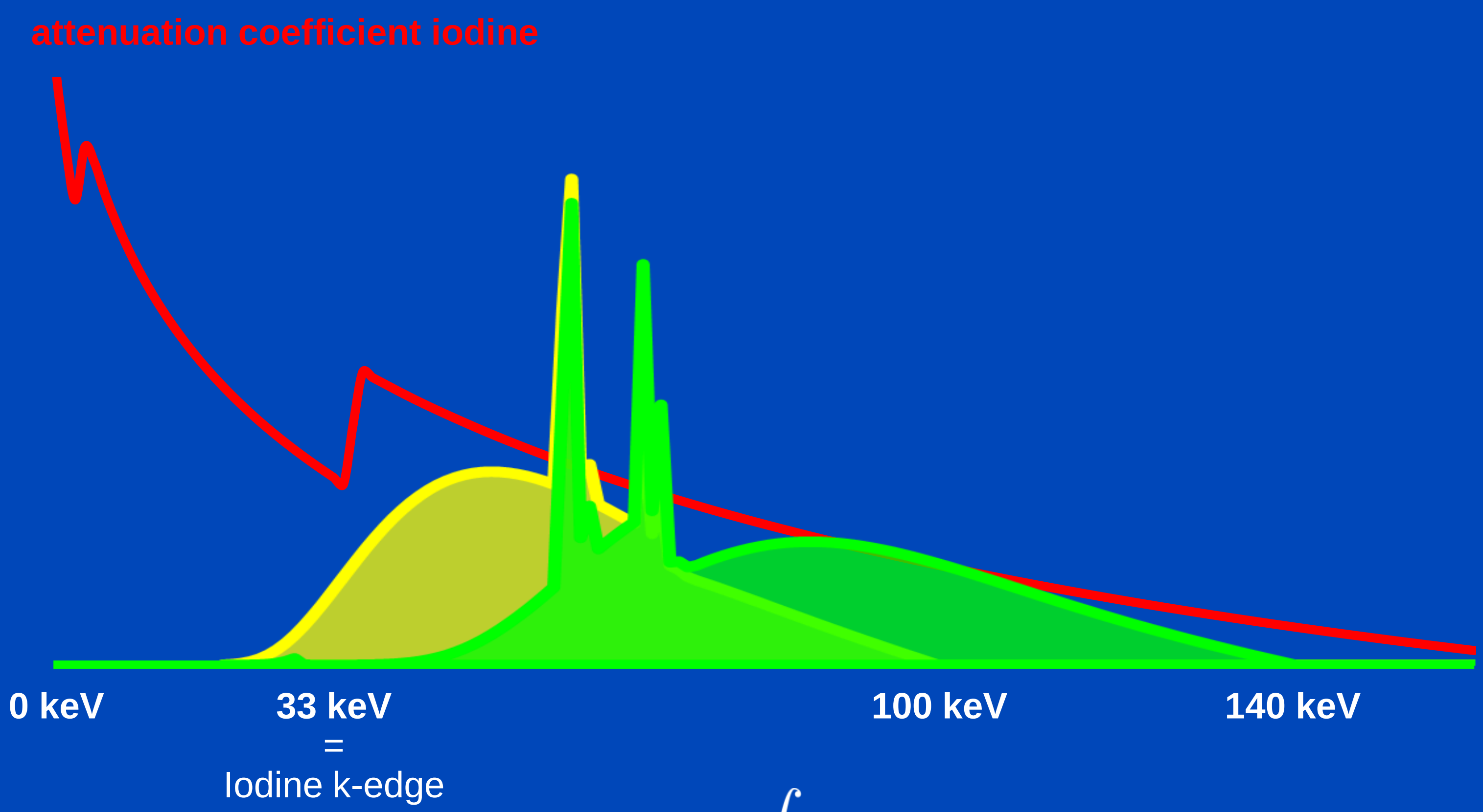

$$\mathrm{Signal}_{\mathrm{PC}} = \int dE\, 1\ N(E)$$

Spectra as seen after having passed a 32 cm water layer.

Iodine CNRD Assessment

Reconstruction Examples @ 80 kV

Small (200 × 300 mm)

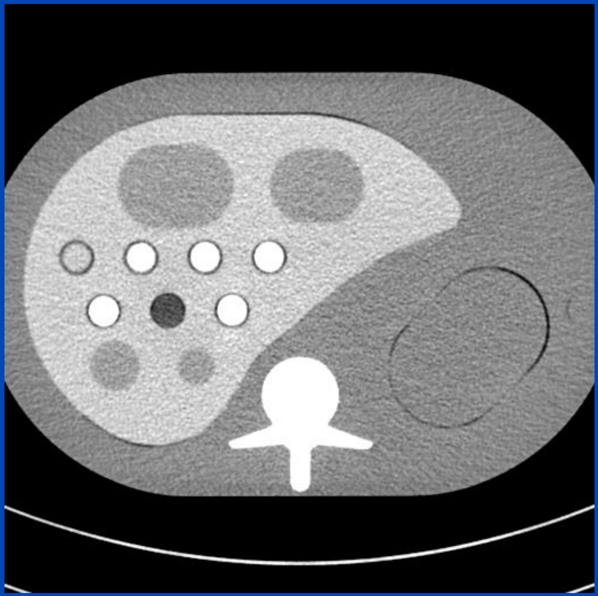

Medium (250 × 350 mm)

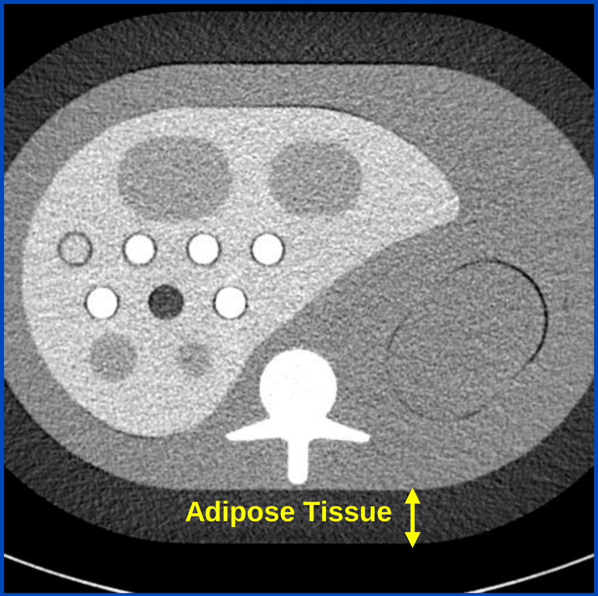

Large (300 × 400 mm)

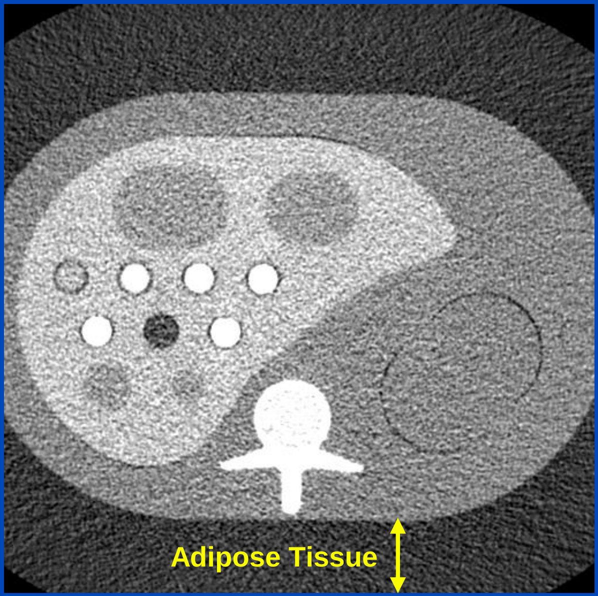

C/W=0 HU/400HU

Iodine CNRD Assessment

Regions of Interest

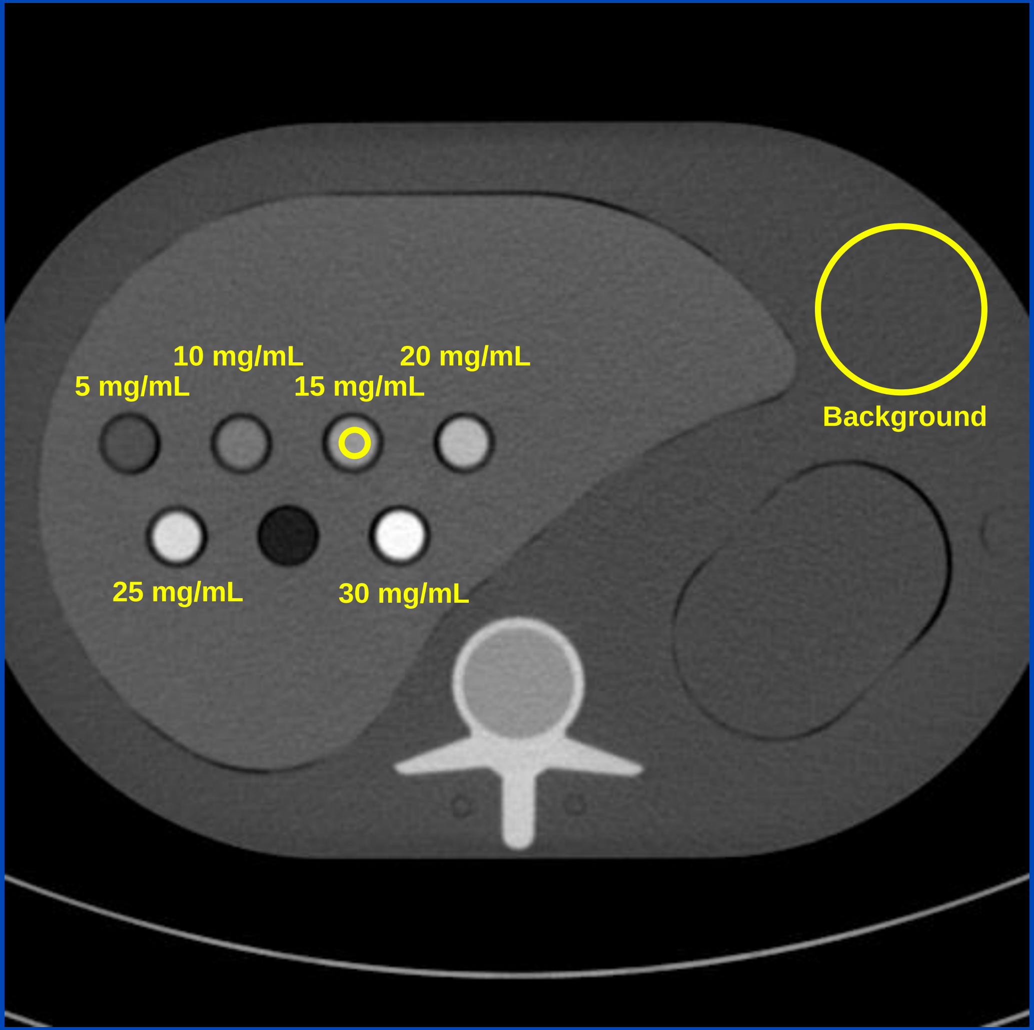

C/W=180 HU/600HU

PC with 1 Bin vs. EI

Potential Dose Reduction

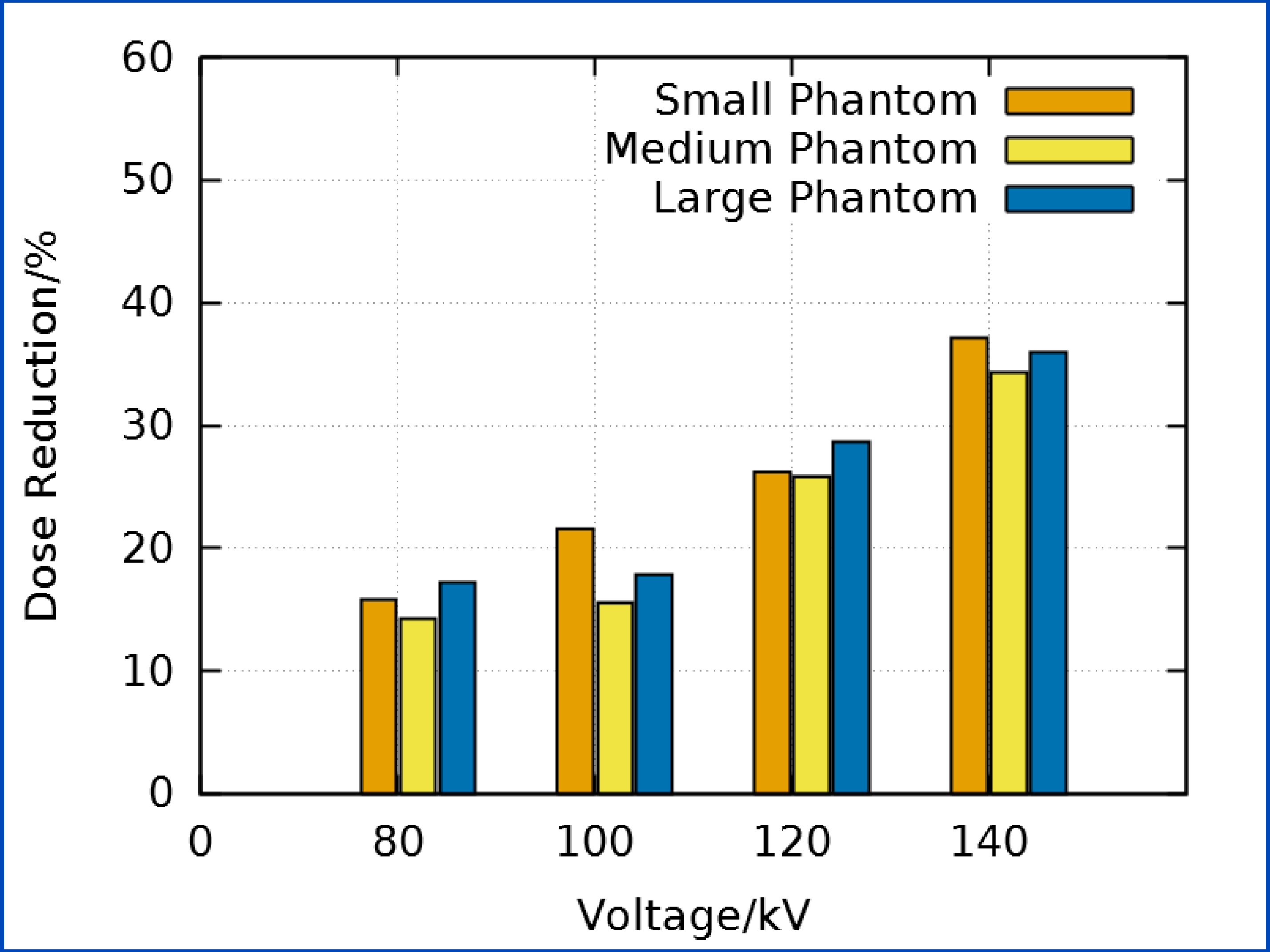

dkfz.

PC with 2 Bins vs. EI

Potential Dose Reduction

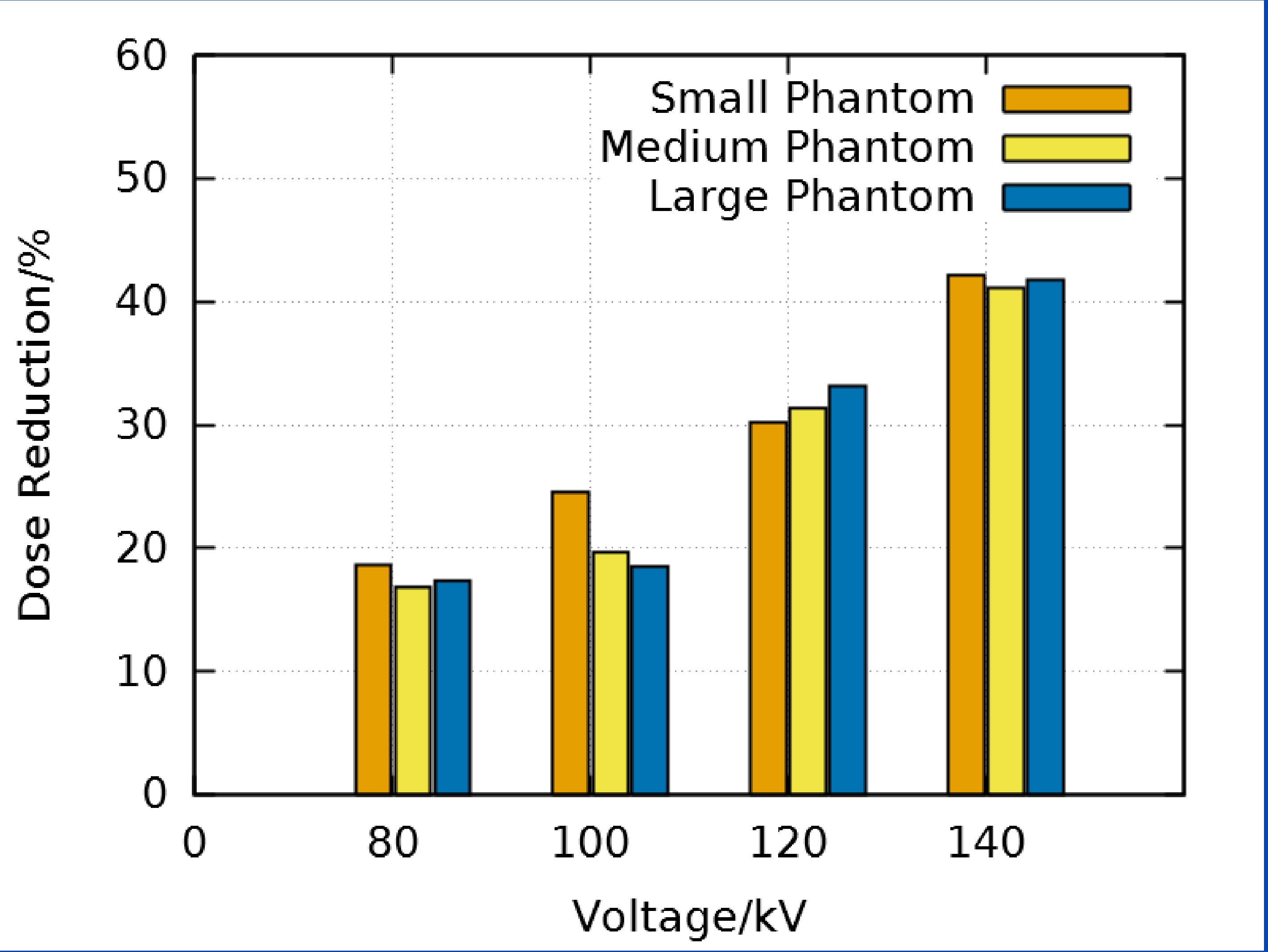

X-Ray Dose Reduction of B70f

PC vs. PC
(“pixel effect only”)

UHR vs. Macro	80 kV	100 kV	120 kV	140 kV
S	**23%** ± 12%	**34%** ± 10%	**35%** ± 11%	**25%** ± 10%
M	**32%** ± 10%	**32%** ± 8%	**35%** ± 8%	**34%** ± 9%
L	**35%** ± 10%	**29%** ± 15%	**27%** ± 9%	**31%** ± 11%

PC vs. EI
(“pixel effect” and “iodine effect”)

UHR vs. EI	80 kV	100 kV	120 kV	140 kV
S	**33%** ± 9%	**52%** ± 5%	**57%** ± 7%	**57%** ± 6%
M	**41%** ± 8%	**47%** ± 7%	**60%** ± 6%	**62%** ± 4%
L	**48%** ± 8%	**43%** ± 10%	**54%** ± 6%	**63%** ± 5%

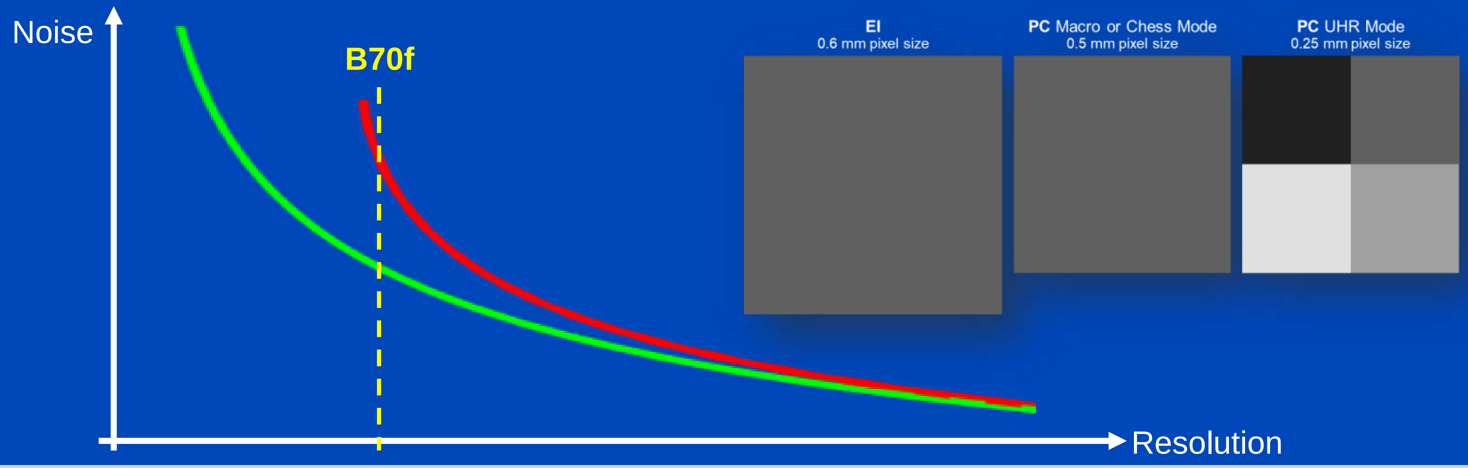

Klein, Kachelrieß, Sawall et al. Invest. Radiol. 55(2), Feb 2020, in press

X-Ray Dose Reduction of D40f

PC vs. PC
(“pixel effect only”)

UHR vs. Macro	80 kV	100 kV	120 kV	140 kV
S	**5%** ± 16%	**12%** ± 17%	**17%** ± 17%	**9%** ± 15%
M	**11%** ± 14%	**9%** ± 12%	**16%** ± 16%	**13%** ± 13%
L	**11%** ± 14%	**6%** ± 17%	**6%** ± 17%	**4%** ± 17%

PC vs. EI
(“pixel effect” and “iodine effect”)

UHR vs. EI	80 kV	100 kV	120 kV	140 kV
S	**10%** ± 11%	**28%** ± 11%	**36%** ± 12%	**38%** ± 12%
M	**15%** ± 12%	**23%** ± 12%	**40%** ± 10%	**43%** ± 9%
L	**24%** ± 14%	**17%** ± 11%	**33%** ± 12%	**43%** ± 9%

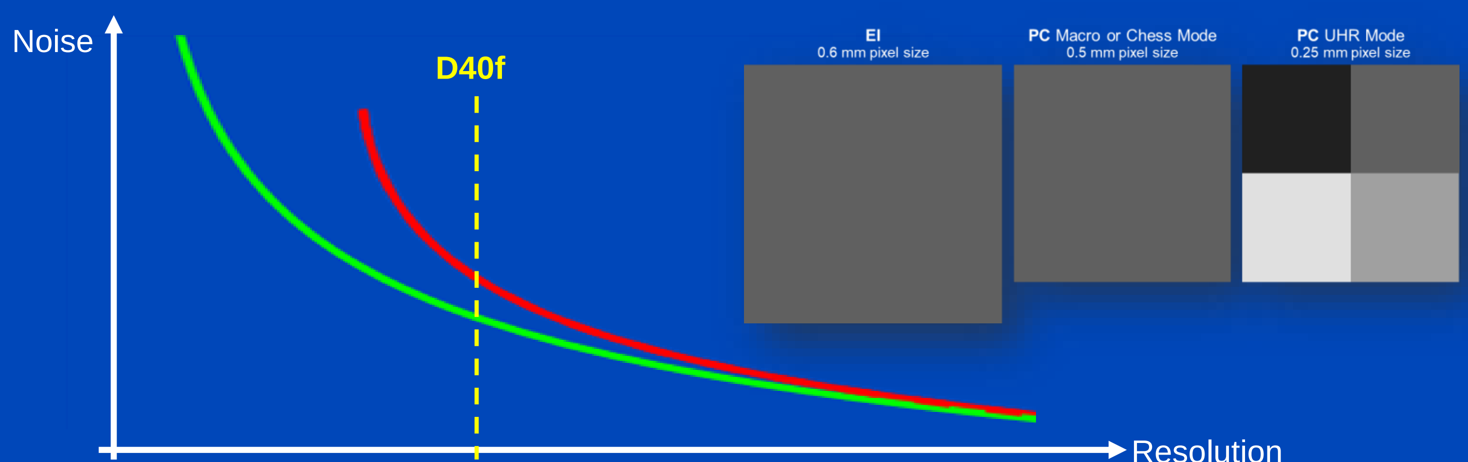

Klein, Kachelrieß, Sawall et al. Invest. Radiol. 55(2), Feb 2020, in press

dkfz.

Conventional reconstruction at spatial resolution of conventional CT (1 mm slices with 0.5 mm pixels)

Iterative reconstruction at spatial resolution of photon counting CT (0.25 mm slices with 0.25 mm pixels)

68 year old woman with breast cancer metastases. $CTDI_{vol}$ = 24.17 mGy, *C* = 500 HU, *W* = 3000 HU.
Images courtesy of the Division of Radiology of the German Cancer Research Center (DKFZ).

dkfz.

MECT

Ca-Gd-I Decomposition

Chess pattern mode
140 kV, 20/35/50/65 keV
C = 0 HU, W = 1200 HU

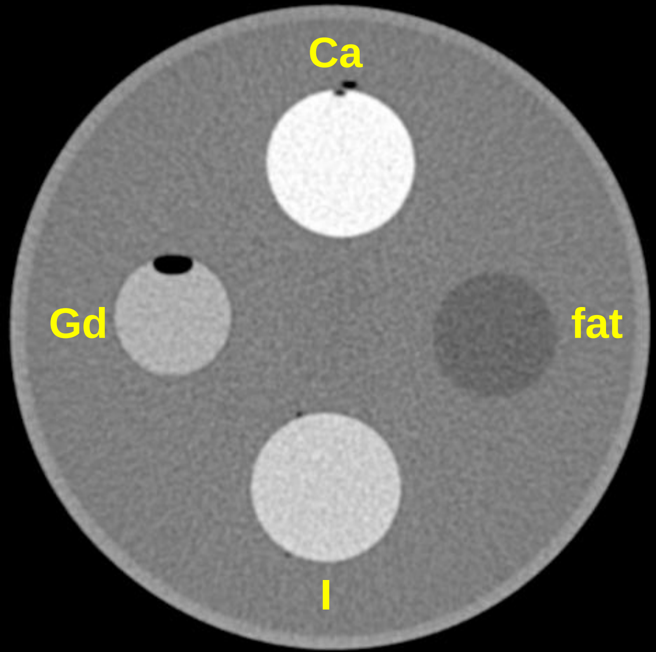

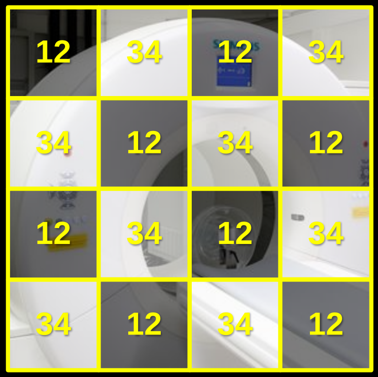

Calcium image

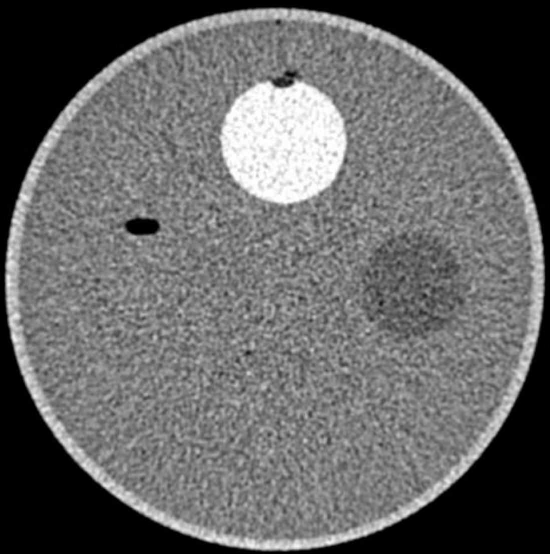

Gadolinium image

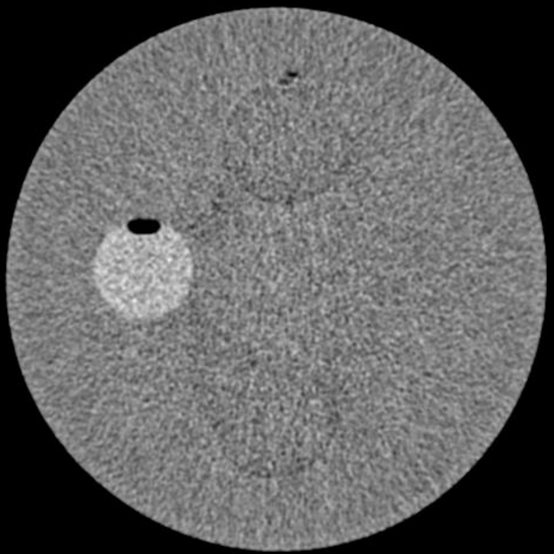

Iodine image

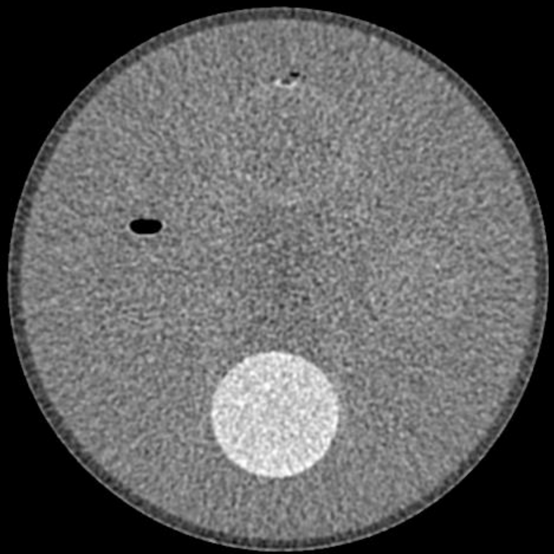

Courtesy of Siemens Healthcare

Summary

- Photon counting CT promises many advantages.
- Several experimental systems have been proposed.
- Clinical data published only for a single experimental photon counting CT (Siemens Somatom CounT)
- More scan modes due to a variety of detector modes
  - Pixel binning
  - Number of thresholds
  - Threshold settings
- Significant improvements expected
  - Higher spatial resolution
  - Spectral information on demand
  - Better dose usage, i.e. less noise, less dose
  - Better image quality
- Clinical product not yet available.

Thank You!

The 6th International Conference on

Image Formation in X-Ray Computed Tomography

August 3 - August 7 • 2020 • Regensburg • Germany • www.ct-meeting.org

Conference Chair: **Marc Kachelrieß**, German Cancer Research Center (DKFZ), Heidelberg, Germany

This presentation is available at www.dkfz.de/ct.
Job opportunities through DKFZ's international Fellowship programs (marc.kachelriess@dkfz.de).
Parts of the reconstruction software were provided by RayConStruct® GmbH, Nürnberg, Germany.